Cubic Defects: Comparing the Eight-State-System with its Two-Level-Approximation

Peter Nalbach, Orestis Terzidis

Institut für theoretische Physik

Philosophenweg 19, 69120 Heidelberg, Germany

February 7, 2008

Abstract

Substitutional defects in a cubic symmetry (such as a lithium defect in a KCl host crystal) can be modeled appropriately by an eight-state-system. Usually this tunneling degree of freedom is approximated by a two-level-system. We investigate the observable differences between the two models in three contexts. First we show that the two models predict different relations between the temperature dependence of specific heat and static susceptibility. Second we demonstrate that in the presence of external forces (pressure and electric field) the eight-state-system shows features that cannot be understood within the framework of the two-level-approximation. In this context we propose an experiment for measuring the parameter for tunneling along the face diagonal. Finally we discuss the differences between the models appearing for strongly coupled pairs. Geometric selection rules and particular forms of asymmetry lead to clear differences between the two models.

1 Introduction

Quantum tunneling of substitutional defect ions in alkali halide crystals leads to particular low temperature properties [1]. Due to their misfit in size or shape such defect ions are confined to a potential energy landscape with a few degenerate potential wells. At low temperatures thermally activated crossing over the barriers is inhibited and the defect ion passes through the barrier by quantum tunneling; typically at a few Kelvin hopping becomes relevant. The potential energy landscape in which the defect ion moves is given by the host crystal and therefore reflects its symmetry which for most alkali halide crystals is cubic (e.g. the fcc-structure of potassium chloride). There are only three multi-well potentials which are consistent with this symmetry: twelve wells at the edges of a cube, six wells in the middle of the surfaces and eight wells at the corners of a cube. In all cases the edges of the cube lie along the crystal

axes and the multi-well structure leads to off-center-sites for the defect ion. The off-center position has two immediate consequences: it separates the centers of charge and leads to a local distortion of the crystal. Hence both an electric dipole moment and an elastic quadrupole moment is connected to the defect which can thus interact with lattice vibrations, external fields or neighboring defects. Consequently only at low defect concentrations one can describe the situation by isolated tunneling systems. With rising concentration pairs, triples etc. of defects are involved until finally one faces a complicated many body system [4, 10].

A standard example of tunneling defects is potassium chloride doped with a small amount of lithium ions (KCl:Li). This system is well described by isolated defects for concentrations up to say 20 ppm. The minima of the system lie on the corners of a cube ($d \approx 1.4$ Å); in the low temperature regime the relevant degree of freedom is thus an eight-state-system (ESS). There are three different matrix elements for tunneling: (i) along the edges of the cube k, (ii) along a face diagonal f and (iii) along a space diagonal r; edge tunneling dominates the defect spectrum [5] for simple geometric reasons: the edge is the shortest distance between the potential minima. Neglecting face and space diagonal tunneling the problem factorizes into three two-level-systems (TLS); this much simpler model is often used for the description of the defect.

In this paper we want to study in how far the TLS is a good approximation for the ESS (and hence in how far tunneling along the face and space diagonal on one hand and the particular geometry of the defect on the other is negligible). We find that in most contexts the TLS approximation is indeed acceptable; still there are quite some experimentally observable features which cannot be explained by the TLS approximation.

The plan of the paper is as follows: In section 2 a tensorial Hamiltonian for the eight-state-system is introduced. Physical properties such as the specific heat and the static dielectric susceptibility are derived and compared with the results of the two-level-approximation. In section 3 we discuss the coupling of the eight-state-system to static external electric or strain fields. We propose an experiment in order to measure directly the parameter for tunneling along a face diagonal. (This parameter will dominate all corrections to the TLS results.) In section 4 strongly coupled pairs of eight-state-systems are considered. We discuss the situation by means of group theory and investigate in particular the relevance of different asymmetry terms for echo experiments. Finally section 5 gives a conclusion.

2 Specific Heat and Static Susceptibility

2.1 Theory

Before going into a discussion of the ESS we would like to summarize some of the well-known features of a TLS. This system describes a particle in a double-well-potential depending on one single coordinate (instead of the three space dimensions of the ESS). The tunneling Hamiltonian of the TLS reads in the 'local' basis (i.e. the basis where σ_z represents the position 'left' or 'right'

of the particle)

$$H = k_0 \sigma_x. \tag{1}$$

The symbols σ_x, σ_z denote the Pauli matrices. The only parameter entering the system is the tunneling parameter k_0 between the left and the right state. It is given by the WKB-formula

$$k_0 = -E_0 \exp\left\{-\frac{d}{2\hbar}\sqrt{2mV_0}\right\} < 0. \tag{2}$$

Here the energy E_0 is the oscillator frequency of a well, d is the distance between the two wells, m is the mass of the tunneling particle and V_0 is the barrier height. Since σ_z represents the position operator, all external fields couple to the product $F\sigma_z$ where F stands for the amplitude of an external field (such as static electric or strain fields and electromagnetic or acoustic waves).

Two characteristic features of the TLS have been studied in numerous experiments: the temperature dependence of the specific heat (Schottky-anomaly)

$$c_v(T) = \frac{k_0^2}{k_B T^2} \quad \mathrm{sech}^2(\beta k_0) \tag{3}$$

and the temperature dependence of the static susceptibility

$$\chi_{stat}(T) = \frac{p^2}{\hbar \epsilon_0} \frac{1}{k_0} \tanh(\beta k_0). \tag{4}$$

Let us now ask: What observable differences appear if we consider the ESS? In order to find an answer we derive the corresponding formulas of this system and compare them to those of the TLS. For the ESS three coordinates determine the wave function in the local basis $\{\,|xyz\rangle\,\}$ with $x, y, z = \pm 1$; the origin of the system is located in the center of the cube and the axes point along its edges. The position operator now becomes a vector

$$\hat{\vec{r}} = \frac{d}{2}\begin{pmatrix} r_x \\ r_y \\ r_z \end{pmatrix} = \frac{d}{2}\begin{pmatrix} \sigma_z \otimes 1 \otimes 1 \\ 1 \otimes \sigma_z \otimes 1 \\ 1 \otimes 1 \otimes \sigma_z \end{pmatrix}, \tag{5}$$

where the symbol $\otimes$ denotes a tensor product and each factor stands for one coordinate. The tunneling Hamiltonian of the ESS can be decomposed into tensor products; edge tunneling along the x–direction for example is described by $k(\sigma_x \otimes 1 \otimes 1)$. Tunneling along the face and space diagonal involves more than one coordinate; the corresponding Hamiltonian is given by

$$\begin{aligned} \hat{H}_0 = \quad & k \quad (1 \otimes 1 \otimes \sigma_x + 1 \otimes \sigma_x \otimes 1 + \sigma_x \otimes 1 \otimes 1) \\ + \quad & f \quad (1 \otimes \sigma_x \otimes \sigma_x + \sigma_x \otimes 1 \otimes \sigma_x + \sigma_x \otimes \sigma_x \otimes 1) \\ + \quad & r \quad (\sigma_x \otimes \sigma_x \otimes \sigma_x). \end{aligned} \tag{6}$$

Here k, f, r are the amplitudes for tunneling along an edge, a face diagonal and a space diagonal. Let us next write down the elastic and electric momenta connected with the defect. The

separation of charge which arises from the off-center-position causes an electric dipole moment

$$\vec{p} = q\vec{r}, \qquad p = \frac{\sqrt{3}}{2} qd. \tag{7}$$

The corresponding interaction energy with an external electric field $\vec{F}$ reads

$$W_F = -\sum_i F_i p_i. \tag{8}$$

Moreover the defect distorts the host crystal locally producing thus an elastic moment. Würger [4] derived as the leading contribution a quadrupole moment

$$Q_{ij} = \frac{4}{d^2} r_i r_j (1 - \delta_{ij}). \tag{9}$$

Remember here that r_i is a component of the position operator. The corresponding interaction energy with a strain field is given by

$$W_\epsilon = -g \sum_{i,j} Q_{ij} \varepsilon_{ij}, \tag{10}$$

where g is a coupling constant and ε_{ij} is the tensor of distortion produced by the strain field. In the static case this tensor can be derived from the exerted pressure using standard elastomechanical relations [3]; in the case of acoustic waves it reads $\varepsilon_{ij} = 1/2(\partial_j u_i + \partial_i u_j)$, where $\vec{u}$ denotes the amplitude of the phonon.

Just as for the TLS the tunneling parameters can be found with the WKB-formula (2). Assuming that the heights of all potential barriers are of the same order of magnitude the three tunneling parameters differ only because of a simple geometric reason: the distance separating the minima is different (the edge of a cube is smaller than a face diagonal etc.). One concludes: $|k| > |f| > |r|$. Hence in a first approach one can neglect f and r. Then the Hamiltonian (6) factorizes and three independent TLS remain, one for each spatial direction. This is nothing else than the two-level-approximation keeping in mind a factor of three: one ESS (with $f = r = 0$) is equivalent to three TLS. One can then conclude: as soon as f and r are not negligible differences between the ESS and the TLS will arise.

Let us go further in our analysis of the ESS. The simple structure of the problem allows the exact calculation of its spectrum and eigenvectors. They are given by the following scheme:

$$\begin{aligned}
E_3 &= -3k + 3f - r \; : && |--\rangle \\
E_2 &= -k - f + r \; : && |+--\rangle, |-+-\rangle, |--+\rangle \\
E_1 &= k - f - r \; : && |++-\rangle, |+-+\rangle, |-++\rangle \\
E_0 &= 3k + 3f + r \; : && |+++\rangle
\end{aligned} \tag{11}$$

with

$$|\pi_x\pi_y\pi_z\rangle = \frac{1}{\sqrt{8}} \sum_{x,y,z=\pm 1} f_x^{\pi_x} f_y^{\pi_y} f_z^{\pi_z} |xyz\rangle \tag{12}$$

$$f_j^{\pi_j} = \exp\left(\frac{i\pi}{4}(1-\pi_j)(1-j)\right). \tag{13}$$

Here $\pi_i = \pm$ denotes the parity of the wave function in the i–direction. The spectrum consists of four levels with a threefold degeneracy of the second and the third level. The transitions shown in figures 1a and 1b are derived from the electric and acoustic interactions given above. As an explicit example we consider an electric field oscillating in the y–direction. Figure 1a gives a complete scheme of the possible transitions.

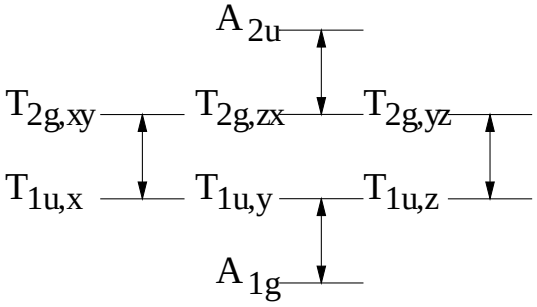

Figure 1a: Selection rules of the ESS for an electric field oscillating in [100]–direction together with the Schoenflies notation.

Every geometric constellation has its specific selection rules; we refrain from giving a complete list of all these possibilities and instead propose in figure 1b a schematic diagram where all possible transitions are shown. Note that for the electric transition one of the parities π_i changes its sign whereas for the acoustic transitions two parities change their signs. Hence in the accoustic case the product $\pi_1\pi_2\pi_3$ is conserved.

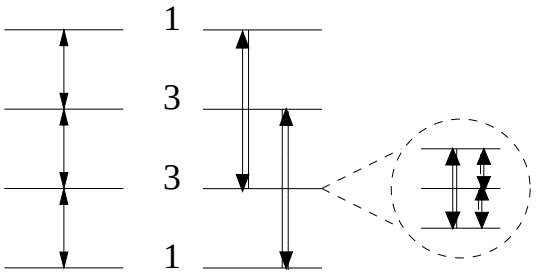

Figure 1b: Possible electric (single arrows) and acoustic (double arrows) selection rules for the ESS

There are three electric transitions with almost the same frequency $\sim 2k$. In the acoustic case there are two transitions with frequency $\sim 4k$ and two 'inside' the degenerate tripletts. (These transitions are visible as soon as some perturbation destroys the degeneracy, cf. section 3). The fact that for both couplings only one transition frequency appears is crucial for the validity of the two-level-approximation: by construction the TLS would not be able to reflect more than

one single energy. Indeed the approximation cannot account for the fact that the frequency induced by electric fields differs from that induced by acoustic fields.

Let us now turn to the temperature dependence of the specific heat and the static susceptibility. The partition function is given by

$$Z = \mathrm{Tr}\left(e^{-\beta H}\right) = \sum_l \eta_l e^{-\beta \mathcal{E}_l} \quad , \quad \beta = \frac{1}{k_B T}$$

where η_l denotes the degree of degeneracy of the eigenvalue $\mathcal{E}_l$ and k_B is the Boltzmann constant. The free energy of the system is then given by $F = -k_B T \ln Z$ and the specific heat reads

$$c_v(T) = \frac{k_B \beta^2}{Z^2} \sum_{i<j} \eta_i \eta_j (\mathcal{E}_i - \mathcal{E}_j)^2 e^{-\beta(\mathcal{E}_i + \mathcal{E}_j)}. \tag{14}$$

Inserting the energies given in (11) one finds for the specific heat of the ESS:

$$\begin{aligned} c_v(T) \;=\; & \frac{k_B \beta^2}{Z^2} \Big\{ (6k+2r)^2 e^{-6\beta f} + 3(4k-4f)^2 e^{-\beta(-2k+2f-2r)} \\ & + 9(2k-2r)^2 e^{2\beta f} + 3(2k-4f+2r)^2 e^{-\beta(-4k+2f)} \\ & + 3(2k+4f+2r)^2 e^{-\beta(4k+2f)} + 3(4k+4f)^2 e^{-\beta(2k+2f+2r)} \Big\}. \end{aligned} \tag{15}$$

This expression reduces to the corresponding formula of the TLS when setting $f = r = 0$.

Let us now write down the susceptibility χ. The response of the ESS to an external field is given by the commutator formula [7]

$$\chi_{ij} = \frac{i}{\hbar} \langle [p_i(t), p_j(t_0)] \rangle \Theta(t - t_0)$$

with the time-dependent dipole operator $p(t) = \exp(i/\hbar \hat{H} t) \hat{p} \exp(-i/\hbar \hat{H} t)$ and the Gibbs mean-value $\langle \cdot \rangle = \mathrm{Tr}(\cdot \exp(-\beta \hat{H}))/Z$. In order to find the static susceptibility one has to look at the real part of the Laplace-transform for zero frequency. This leads to

$$\begin{aligned} \chi^{stat}_{x,x}(T) = \frac{2}{Z} \frac{p^2}{\hbar \epsilon_0} \Big\{ & \left[e^{\beta(3k+3f+r)} - e^{-\beta(k-f-r)} \right] \frac{1}{(2k+4f+2r)} \\ + \; & 2 \left[e^{\beta(k+f-r)} - e^{-\beta(-k-f+r)} \right] \frac{1}{(2k-2r)} \\ + \; & \left[e^{-\beta(-k-f+r)} - e^{\beta(-3k+3f-r)} \right] \frac{1}{(2k-4f+2r)} \Big\}. \end{aligned} \tag{16}$$

All other elements of the susceptibility tensor are then known: the symmetry of the problem implies $\chi_{x,x} = \chi_{y,y} = \chi_{z,z}$ and $\chi_{x,y} = \chi_{x,z} = \chi_{y,z} = 0$. Again this result reduces to the corresponding formula for the TLS in the case of vanishing face and space diagonal parameters.

At first sight almost no contrast between the two models emerges from the above formulas. Taking reasonable values for f and r (say $r/f = f/k \approx 10 - 20\%$), the plots look practically the same. The question arises whether there is at all a simple observable feature which distinguishes between the TLS and the ESS. Indeed such a criterion exists. It is based on the observation that

for the TLS the relation $k_0^2 \partial_T \chi = c_V$ holds, whereas this is not true for the ESS. One simple consequence is that the turning point of the susceptibility and the maximum of the specific heat *coincide* for a TLS, whereas they occur at *different* temperatures for the ESS. To be more explicit: Defining

$$\begin{aligned} T_{max}: \quad & \tfrac{\partial}{\partial T} c_V(T = T_{max}) \quad = 0 \\ T_{turn}: \quad & \tfrac{\partial^2}{\partial T^2} c_V(T = T_{turn}) \quad = 0 \end{aligned} \tag{17}$$

one finds for the TLS

$$T_{max} = T_{turn},$$

whereas for the ESS

$$T_{max} < T_{turn} \tag{18}$$

holds. It is not possible to give an explicit expression of $\Delta T = T_{turn} - T_{max}$ as a function of f and k since transcendental equations are involved. Instead we plot in figure 2 ΔT as a function of f with parameter k. It turns out that ΔT depends only very weakly on k for $0.5K < |k|/k_B < 1.5K$ and that a linear relation $\Delta T \approx 0.85\ |f|/k_B$ holds approximately.

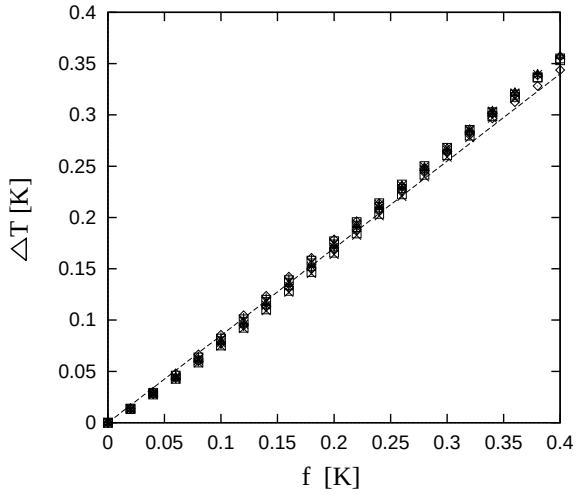

Figure 2: $\Delta T = T_{turn} - T_{max}$ as a function of $|f|$. The different points indicate different values of $|k|$ between 0.5 and 1.5 Kelvin. The line is a linear fit with a slope of 0.85

As the ESS is the more realistic model the deviation $T_{max} \neq T_{turn}$ should be visible in experiments. This will be discussed in the following.

Note that Fiory [8] has shown that even for low concentrations the 'Schottky anomaly' of the specific heat gets distorted by the dipole–dipole–interaction between the defects, and a similiar effect is expected for the dielectric susceptibility. Both effects - the interaction and face tunneling - might interfer in a real sample. But by examing probes with different defect concentrations it is in principle possible to distinguish between the two effects; any change depending on a variation of concentration results from interactions while effects that are independent from such a variation arise due to face diagonal tunneling.

2.2 Experimental Data

Let us now take a look at the experimental data. We will make use of the specific heat data from Pohl et al. [2] and the dielectric susceptibility data from Enss et al. [6]. Since f will be the leading correction to the TLS approximation we will neglect r in the following. We then have two fit parameters f and k and we can look for the optimal set in order to reproduce the data. But indeed there is a third undetermined quantity: the defect concentration of the probe cannot be fixed accurately. But the concentration varies only in a very small range so we focus on the tunneling parameters. All parameter sets consistent with experimental data (obtained by fitting the relations 15 and 16 to the data) indeed confirm the relation $T_{max} < T_{turn}$.

For a further comparison of the two models we will proceed as follows. The TLS is completely specified by the parameter k_0 whereas the ESS is specified by the pair (k, f). Now one can ask: What relation between the ESS parameter pair (k, f) and the single TLS parameter k_0 must hold in order to produce either the same maximum of c_v or the same turning point of χ ? The c_V-maxima of the two models coincide if the equation $k + 1.7f \approx k_0$ is fulfilled (which can be verified by differentiating and solving a transcendental equation). The turning points of χ are the same if $k + 2.7f \approx k_0$ holds. This shows that an TLS-analysis yields indeed different tunneling parameters for the two experiments which is counterintuitive; after all the same degree of freedom produces both anomalies. Usually such effects were thought to be due to experimental uncertainty; but the above considerations show that the difference is a systematic consequence of tunneling along the face diagonal. Based on the difference between T_{max} and T_{turn} one can estimate an optimal parameter set. In order to do so one has to solve a set of transcendental equations, where T_{max} and T_{turn} are given by the data and f and k are the unknown variables. We have listed the result in table 1.

	^6Li	^7Li
k/k_B	$-0.63K$	$-0.45K$
f/k_B	$-0.08K$	$-0.06K$
$c_v \ : \ (k + 1.7f)/k_B$	$-0.77K$	$-0.55K$
$\chi \ : \ (k + 2.7f)/k_B$	$-0.85K$	$-0.61K$

Table 1: Parameter set consistent with experimental data. In the lower part of the table effective values for a TLS are listed.

At first sight the results for k look smaller than these reported in the literature. But keep in mind that most experiments so far were fitted by a TLS approach. Therefore we have also listed such 'effective' parameters emerging from an equivalent fit within the TLS model. These values are in line with those reported by other authors. The above parameter set is also in good

agreement with restrictions arising from the WKB-formula (2). Then corresponding restrictions concern both the ratio

$$\frac{f}{k} = \exp\left\{-\frac{\sqrt{2mV_0}}{2\hbar}d(\sqrt{2}-1)\right\} \tag{19}$$

and the ratio of the isotope effect:

$$\frac{{}^6k}{{}^7k} = \exp\left\{-\frac{d\sqrt{2V_0}}{2\hbar}(\sqrt{{}^6m}-\sqrt{{}^7m})\right\}. \tag{20}$$

The tunneling distance $d \approx 1.4$Å and the mass m of the lithium are known; the barrier height V_0 between all wells should be of the same order of magnitude. The ratios proposed above ($f/k \approx 0.13$ and ${}^6k/\,{}^7k \approx 1.4$) are then consistent with $V_0 \approx 200$ K and $V_0 \approx 140$ K respectively. This seems a rather reasonable value for the barrier height. So the above given parameter set is at least consistent with the given data. We would not like to go further than this statement, but only stress, that the ESS is not in contradiction with experimental data. Furthermore it reflects much better the microscopic picture we have in mind when talking about a substitutional defect. Still the TLS seems useful: it has almost the same temperature dependence of specific heat and static susceptibility and is of course much simpler. Nevertheless there appear some aspects which the TLS cannot reproduce at all. In the following we will discuss these aspects. In section 3 such properties arise from the tunneling parameters f and r; we will show that these features make it possible to measure the tunneling parameters directly. The properties described in section 4 are based on the particular geometric structure of the ESS; this structure leads to selection rules which cannot be understood in the framework of a one-dimensional model such as the TLS.

3 Interaction with External Fields

As mentioned above the defects exhibit both electric and elastic moments; they hence couple to the corresponding external fields. The main effect of static fields is a modification of the energy levels, whereas oscillating fields lead to characteristic transition rules. We will discuss the features in three steps: first we look at the defect under pressure and second under the influence of a static electric field. For both cases we look at the field dependence and the selection rules for transitions induced by acoustic and electromagnetic waves. Based on these results we finally propose an experiment which can determine the tunneling parameter f (face diagonal tunneling). Indeed in section 3.1 and 3.2 we will focus on situations where f becomes visible.

3.1 The Defect under Pressure

Let us begin by considering a defect under the influence of external pressure. As discussed before (see eq. (9)) the defect exhibits an elastic quadrupole moment $Q_{ij} \propto r_i r_j(1-\delta_{ij})$ which

interacts with the strain field ε_{ij}. The latter can be derived by elastomechanical equations from the pressure exerted on the system [3]. The interaction energy (cf. sect. 2) reads $W_\varepsilon = -g\sum_{ij} Q_{ij}\varepsilon_{ij}$. Since Q_{ij} has (by definition) no diagonal part, the diagonal part of the strain field is irrelevant for the interaction. This fact simplifies the discussion considerably: the diagonal part of the strain field depends on the pressure in a rather non-trivial way.

The energy eigenvalue problem of a defect in an arbitrary strain field (i.e. uniaxial pressure in an arbitrary direction) is not analytically solvable. Yet some constellations with high symmetry can be solved by means of group theory. Such tractable cases appear for uniaxial pressure in [100]–, [110]– and [111]–direction. Let us write down the interaction hamiltonian for these cases. In order to do so one has to derive the strain field which arises from the exerted pressure [3]. For the cases we consider these strain fields and the corresponding interaction energies are listed in table 2.

direction of uniaxial pressure	distortion field $\boldsymbol{\varepsilon}$	interaction energy W_ϵ
[001]	$\varepsilon_{ij} = \begin{pmatrix} \varepsilon_1 & 0 & 0 \\ 0 & \varepsilon_2 & 0 \\ 0 & 0 & \varepsilon_2 \end{pmatrix}$	0
[011]	$\varepsilon_{ij} = \begin{pmatrix} \varepsilon_1 & 0 & 0 \\ 0 & \varepsilon_2 & \varepsilon \\ 0 & \varepsilon & \varepsilon_2 \end{pmatrix}$	$-\frac{4g\varepsilon}{d^2}(1\otimes\sigma_z\otimes\sigma_z)$
[111]	$\varepsilon_{ij} = \begin{pmatrix} \varepsilon_1 & \varepsilon & \varepsilon \\ \varepsilon & \varepsilon_1 & \varepsilon \\ \varepsilon & \varepsilon & \varepsilon_1 \end{pmatrix}$	$-\frac{4g\varepsilon}{d^2}(1\otimes\sigma_z\otimes\sigma_z + \sigma_z\otimes 1\otimes\sigma_z + \sigma_z\otimes\sigma_z\otimes 1)$

Table 2: Distortion field and interaction energy for different directions

The off-diagonal elements ε of the strain fields are proportional to the pressure; the proportionality factor depends on the crystal's elasticity modulus. The case of exerting pressure in the [100]–direction turns out to be trivial since the strain field then has no off-diagonal elements and the interaction energy thus vanishes. The eigenvalue problem of the other two cases have been discussed in a two-level-approximation (i.e. $f = r = 0$) by Gomez et al. [5]. We want to avoid this approximation and focus on the case where the pressure is exerted in the [110]–direction (a general discussion can be found in [12]). In this situation the Hamiltonian of a defect under uniaxial pressure reads

$$H = H_0 - \frac{4g\varepsilon}{d^2}(1\otimes\sigma_z\otimes\sigma_z). \tag{21}$$

We will not write down any formulas concerning the eigenvalues and -vectors (which can be found in reference [12]); instead we will plot all interesting information and give a discussion.

Figure 3 shows the dependence of the energy levels on the pressure. The energies E3, E4, E5 and E6 grow linearly with pressure; the others vary quadratically for small pressure and then end up in a linear regime. All degeneracies are obviously lifted. With growing pressure the spectrum changes from four almost equidistant levels to four dubletts; the energy difference inside such a dublett is asymptotically of the order of f. The upper two dubletts are separated by a gap from the lower two; this gap varies (asymptotically) linearly with pressure whereas the distance of the dublett splitting approaches $\sim 2k$.

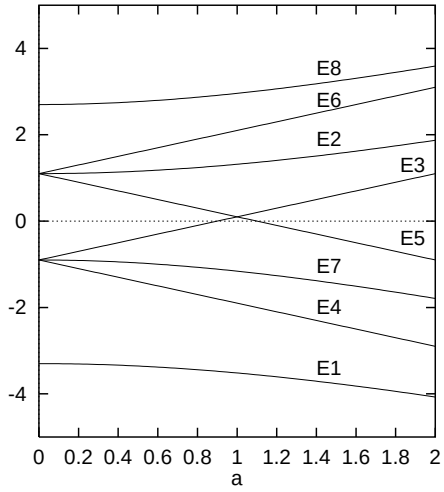

Figure 3: Energy levels of an ESS (in units of k) versus $a = 4g\varepsilon/d^2$ which is proportional to the uniaxial pressure in [110]–direction

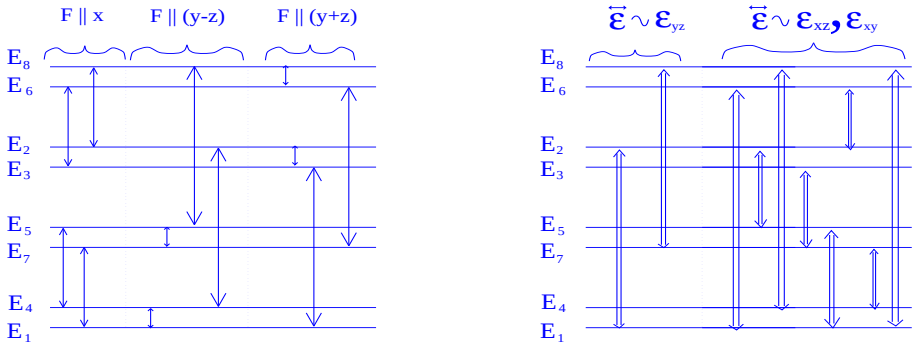

Figure 4: Energy levels of an ESS with uniaxial pressure in [110]–direction and the electric (left picture, single arrows) and acoustic (right picture, double arrows) transitions

Figure 4 shows the possible electromagnetic and acoustic transitions; the pressure is chosen such that the coupling energy is roughly the same as the tunneling energy. In the left part of the scheme simple arrows indicate a dipole transition (microwaves) and in the right part double arrows denote quadrupole transitions (acoustic waves). The symbol $\vec{F}$ here stands for the electric field of the electromagnetic wave and $\boldsymbol{\varepsilon}$ for the (symmetric) distortion field of the acoustic wave (with $\epsilon_{ij} = 1$ for row index i and column index j). The scheme shows that most transitions can be induced by an appropriate choice of the direction of the oscillating fields; in particular the frequency $\sim f$ can be induced by a microwave field with $\vec{F}$ oscillating in the [110]

direction.

3.2 The Defect in the Presence of a Static Electric Field

Let us now consider the defect in a static electric field (cf. eq. (7)). The coupling energy between the field and the defect reads $W_F = -\sum_i F_i p_i$. Again the general situation of a defect in an electric field of arbitrary direction is not analytically solvable. Two possible restrictions allow such a solution. One of them is to neglect f and r; in this 'two-level-approximation' the Hamiltonian $\hat{H} = \hat{H}_0 - \vec{F}\vec{r}$ factorizes into three two-dimensional problems. It is then easy to derive the spectrum and the transitions. This has been done by Gomez et al. [5] for special symmetries, but it is in fact possible for arbitrary directions of the electric field. The second possibility is to consider cases where the electric field points along the [100]–, [110]– and [111]–direction. The resulting problem then still has a high symmetry and group theory makes it possible to find a solution even for finite f and r. The interesting new feature emerging is the occurrence of transition frequencies proportional to f (neglecting r) in the [110]– and [111]–cases. These transitions are interesting since they allow a direct measurement of f (which will be discussed below). We will consider the [111]–case here; the others can be found in reference [12].

The Hamiltonian for a defect with an electric field in [111]–direction reads

$$\begin{aligned} H_{(111)} &= k\,(1\otimes 1\otimes\sigma_x + 1\otimes\sigma_x\otimes 1 + \sigma_x\otimes 1\otimes 1) \\ &+ f\,(1\otimes\sigma_x\otimes\sigma_x + \sigma_x\otimes 1\otimes\sigma_x + \sigma_x\otimes\sigma_x\otimes 1) \\ &+ r\,(\sigma_x\otimes\sigma_x\otimes\sigma_x) \\ &- q\tfrac{d}{2}F_{stat}\,(1\otimes 1\otimes\sigma_z + 1\otimes\sigma_z\otimes 1 + \sigma_z\otimes 1\otimes 1). \end{aligned} \tag{22}$$

The presence of the exterior field breaks the cubic symmetry (O_H) of the defect. In the case considered one is left with the so-called C_{3v}–symmetry group (i.e. there is one threefold axes and three vertical reflection planes). Group theory then shows that the spectrum consists of four singletts and two dubletts since the eight-dimensional representation decomposes into four one-dimensional and two two-dimensional irreducible representations. Correspondingly it is possible to blockdiagonalize the Hamiltonian. These blocks can then be treated in (degenerate) perturbation theory since $f, r \ll k, pF$. Again we refrain from writing down details and instead restrict ourselves to a discussion of the results. In figure 5 the eigenvalues are plotted against the static field F_{stat}. In contrast to the level shift due to pressure there is no linear field dependence of any energy level. Neglecting f and r the spectrum conserves the $1:3:3:1$ degeneracy scheme. The four levels simply spread with increasing field as $2\sqrt{k^2 + (qdF/2)^2}$. Considering finite f and r changes the situation. The most remarkable new feature is the splitting of the threefold degenerate states into a singlett (E_1,E_2) and a dublett (E_5,E_6). This splitting is

proportional to the face diagonal tunneling parameter f; it is given by

$$E_1 - E_5 = E_2 - E_6 = f\,\frac{3(pF/\sqrt{3})^2}{(pF/\sqrt{3})^2 + k^2}. \tag{23}$$

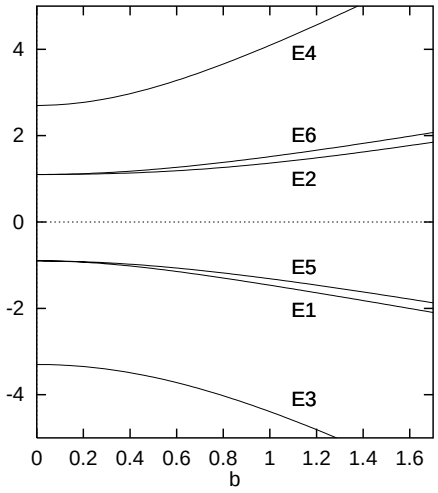

Figure 5: Energy levels of an ESS (in units of k) versus $b = pF/\sqrt{3}|k|$ which is essentially the static electric field in [111]–direction

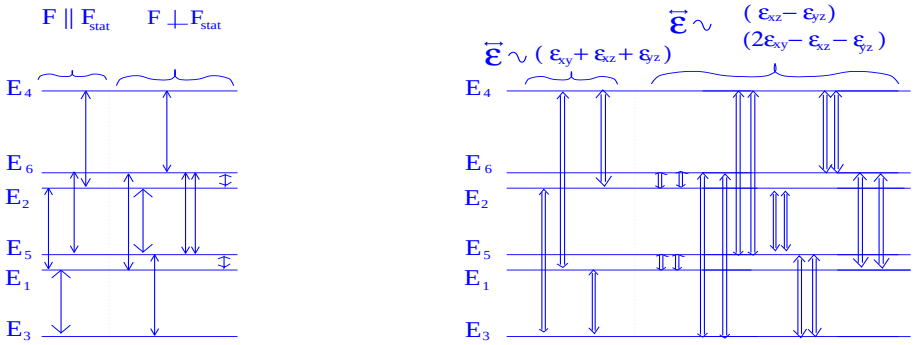

Figure 6: Energy levels of an ESS with electric field in [111]–direction and the electric (left picture, single arrows) and acoustic (right picture, double arrows) transitions

Figure 6 gives the transition scheme of the situation. In the left part of the scheme we again show the dipole transitions. Two cases are listed: one where the electric field of the microwaves oscillates in line with the static field and one where it oscillates in a perpendicular direction.

Suppressing amplitudes $\propto |f/k|^2$ we find in the first case four transitions: the selection rules remain essentially unaltered and lead to transitions of the order of $\sim 2k$. If the oscillating field is perpendicular to the static field many transitions are possible: those 'over the gap' with a frequency growing with increasing static field as well as those taking place 'inside' a triplett. The frequency of the latter is asymptotically determined by f. The probability for the dipole transition grows with the amplitude of the static field $\propto F_{stat}^2$.

The acoustic selection rules are shown in the right part of figure 6. There is a whole variety of possible transitions; again we want to focus on the one with frequency f. The distortion tensor

ε_{ij} for such a transition has to be proportional to $a_1(2\epsilon_{xy}-\epsilon_{xz}-\epsilon_{yz})+a_2(\epsilon_{xz}-\epsilon_{yz})$ with arbitrary a_i. One possible choice is a sound wave propagating along the $(y-z)$-direction being polarized in the x-direction. The transition amplitude of such a constellation is given by $\left|\frac{k^2-2(qdF_{stat}/2)^2}{k^2+2(qdF_{stat}/2)^2}\right|^2$. The increasing static field reduces the amplitude which vanishes for $F_{stat}=\sqrt{2}kqd$. For coupling energies greater than the tunneling energy the transition probability then again increases.

3.3 Measuring Face Diagonal Tunneling

The results of the preceding sections show that there are different possibilities to measure the face diagonal tunneling parameter by choosing an appropriate geometric constellation for the exterior static and oscillating fields. Let us focus in the following on the situation of a static electric field pointing along the [111]–direction (cf. section 3.2). The electric field of the microwave is assumed to oscillate perpendicular to the static field (for example in the [0,1,-1]–direction). The selection rules tell us that a transition with frequency $\sim f$ (which should be about 100mK) is possible. In order to have a transition rate of the order of unity, one has to apply a static field which leads to an interaction energy of the order of k. This is fulfilled if $pF\approx k$. Since the dipole moment of the defect is known to be $p\approx 2.6D$ and $k\approx 1$K (cf. [4]), the field strength should be $F_{stat}\approx 10^6-10^7$V/m. To our knowledge such an experiment has never been performed.

4 Strongly Coupled Pairs

In section 2 we argued that a substitutional defect exhibits an electric as well as an elastic moment. These momenta lead to a coupling of the defects to external fields; moreover they produce an interaction between neighboring defects. Here again both are present, the quadrupole coupling of the elastic moments and the dipole-dipole-coupling of the electric moments. In potassium chloride doped with lithium the electric interaction dominates the elastic coupling by an order of magnitude. Hence only the dipole–dipole interaction

$$W=\frac{1}{4\pi\varepsilon\varepsilon_0}\left(\frac{\vec{p_1}\vec{p_2}}{R^3}-3\frac{(\vec{p_1}\vec{R})(\vec{p_2}\vec{R})}{R^5}\right)=\frac{J}{4}\left(\vec{e}_1\vec{e}_2-3(\vec{e}_1\vec{e}_R)(\vec{e}_2\vec{e}_R)\right) \tag{24}$$

with

$$J=\frac{1}{\pi\varepsilon\varepsilon_0 R^3}\frac{p^2}{3} \tag{25}$$

is relevant. Here $\vec{p}_i$ denotes the dipole moment of defect i, $\vec{R}$ is the vector connecting the defects, the $\vec{e}$'s are $\vec{e}=(2/d)\vec{r}$, ε_0 and ε are the dielectric constant of the vacuum and the potassium chloride matrix respectively.

The structure of the host crystal confines the defects to discrete sites on the lattice. Hence the possible distances between the pairs will be a discrete set. Although this fact is irrelevant for the bulk of the pairs which have a distance of, say, ten lattice constants or more (the crystal then appears as a quasicontinuum), it is most relevant for the strongly coupled pairs which we

will consider here. Geometric considerations show that on the fcc lattice the nearest neighbors NN1 lie along the [1/2,1/2 ,0]-directions and the next nearest neighbors NN2 along the [1,0,0]-direction. Comparing the energy scales for neighboring pairs one finds that the interaction energy dominates the ESS tunneling parameters. This can be estimated by evaluating the dipole–dipole interaction (24) using the lattice constant $a \approx 6.23$Å and the dipole moment $p \approx 2.6D$. For the nearest neighbors NN1 one is lead to a value of $\varepsilon J \approx 710$K (evaluated with $R = a/\sqrt{2}$). In order to determine the value of the coupling one has to specify the dielectric constant of the material. Yet on the atomic length scale it is not clear which value to take for this constant; at least one can confine it to the interval $\varepsilon(\text{vacuum}) = 1 < \varepsilon < \varepsilon(\text{KCl}) = 4.25$. This tolerence leads to values $170\,K < J_{NN1}/k_B < 710\,K$. For the next nearest neighbors NN2 the interval is $60\,K < J_{NN2}/k_B < 250\,K$. This estimation, as rough as it is, shows that the coupling between neighboring defects exceeds by at least one order of magnitude the intrinsic energy scales (which are given by $k \approx 1$K). The strongly coupled pairs hence constitute a composite degree of freedom which should be considered as a unit.

Klein [11] and one of the authors [10] have discussed defect pairs in the two-level-approximation; within this approximation one can predict the existence of a small frequency $4k^2/J$ for strongly coupled pairs. For nearest or next nearest neighbors this energy should be between 5mK and 50mK. Weis et al. [9] investigated the system experimentally by measuring Rabi frequencies in spin echo experiments. He found a broad distribution of frequencies in the 10mK region; in addition there was a rather narrow distribution of Rabi frequencies $\Omega_R \propto \frac{4k^2/J}{E}\,\vec{F}\vec{p}$. The analysis of these experiments was first done by considering the strongly coupled pair as an effective TLS with a tunneling rate $4k^2/J$ and an asymmetry Δ. The total energy of such an effective TLS then reads $E = \sqrt{\Delta^2 + (4k^2/J)^2}$ (which is the resonance energy of the external field). Weis now argued that the measured frequency distribution is due to a distribution of the asymmetry Δ. Such a distribution arises from imperfections of the probe, whereas there is no plausible reason for a distribution of the dipole moment.

Still the existence of only one frequency was somehow striking; obviously only one pair constellation contributed to the signal (otherwise additional Rabi frequency peaks would appear). In order to explain this puzzle Würger [4] discussed a pair of ESS using perturbation theory. He showed that only the pair constellation NN2 has a frequency in the range between 5mK and 50mK. For all other constellations geometric selection rules prohibit transitions with these energies. He also showed that an asymmetry proportional to the position operator explains the distribution of frequencies. Yet he left open the question which role other forms of asymmetries (e.g. a 'quadrupole asymmetry' proportional to $r_i r_j$ which couples to internal strain fields) will play.

In order to treat this problem one can discuss the NN1 and NN2 case applying group theory and tensor factorization. In this context all types of asymmetries are easily discussed considering them as small perturbations. We restrict ourselves to a brief overview of the proposed methods and present the results for the NN2 constellation (for details cf. [12]).

First the basis $\{\,|xyz\rangle\,\}$ for one defect is expanded to $\{\,|x_1x_2y_1y_2z_1z_2\rangle\,\}$ for the pair. In this basis the Hamiltonian reads

$$H = H_0 + W \tag{26}$$

where H_0 stands for the tunneling energy of both defects and W denotes the dipole interaction. This (64-dimensional) Hamiltonian indeed factorizes just as in the case of a single defect (we write k_i for the edge tunneling rate of the defect i):

$$\begin{aligned} H \;=\; & \Big(k_1(\sigma_x\otimes 1) + k_2(1\otimes\sigma_x) - \frac{J}{2}(\sigma_z\otimes\sigma_z)\Big)\otimes \mathbf{1}_{4\otimes 4}\otimes \mathbf{1}_{4\otimes 4} \\ & + \mathbf{1}_{4\otimes 4}\otimes\Big(k_1(\sigma_x\otimes 1) + k_2(1\otimes\sigma_x) + \frac{J}{4}(\sigma_z\otimes\sigma_z)\Big)\otimes \mathbf{1}_{4\otimes 4} \\ & + \mathbf{1}_{4\otimes 4}\otimes \mathbf{1}_{4\otimes 4}\otimes\Big(k_1(\sigma_x\otimes 1) + k_2(1\otimes\sigma_x) + \frac{J}{4}(\sigma_z\otimes\sigma_z)\Big). \end{aligned} \tag{27}$$

We are left with three four-dimensional problems. After this factorization it is easy to derive the complete spectrum together with all selection rules. This spectrum consists of different multipletts which are separated by gaps of the order of $\sim \frac{J}{4}$. For the experiments considered the temperature is much lower than this energy and hence only the lowest level group is of interest. In the middle of figure 7 the spectrum of this lowest multiplett is shown together with the dipole selection rules. It consists of eight states with a degeneracy scheme $1:1:2:2:1:1$. The energy eigenvalues are typically the sum of three roots of the form $\sqrt{(J/4)^2+(k_1\pm k_2)^2}$ and $\sqrt{(J/2)^2+(k_1\pm k_2)^2}$.

In order to determine the transitions caused by an external field one has to consider an interaction with both defects: $W_F = -\vec{F}(\vec{p}_1+\vec{p}_2)$. The spatial dependence of F is neglected since the wavelength of F ($\approx$ 1cm) is much greater than the distance of the two defects ($\approx$ 10Å). There is only one transition frequency (just as in the case of a single defect). But here transitions are only induced by electric fields $\vec{F}$ oscillating in line with the distance vector $\vec{R}$.

The structure of the spectrum together with the selection rules makes it again possible to talk about the pair as an effective TLS with tunneling rate $4k_1k_2/J$. In particular it is possible to use the well-known Rabi-formalism for TLS in order to interpret the echo experiments. In a way this is an a posteriori justification of the TLS approximation which had been proposed in the context of defect pairs [10].

Considering now an asymmetry is somewhat more complicated as in the two-level-approximation. There the asymmetry is simply proportional to the one-dimensional position operator. The ESS is in a sense three-dimensional and one has to find a way to assign a different potential value to each well. This can be done by introducing three dipole terms, three quadrupole terms and an octupole term. Allowing different asymmetries at both defects one gets:

$$V_d \;=\; \sum_{i=x,y,z} v_i(r_i^1+r_i^2) + \delta v_i(r_i^1-r_i^2) \tag{28}$$

$$V_q \;=\; \sum_{\substack{i,j=x,y,z\\ i\neq j}} v_{ij}(r_i^1r_j^1+r_i^2r_j^2) + \delta v_{ij}(r_i^1r_j^1-r_i^2r_j^2) \tag{29}$$

$$V_o \;=\; v_{xyz}(r_x^1r_y^1r_z^1+r_x^2r_y^2r_z^2) + \delta v_{xyz}(r_x^1r_y^1r_z^1-r_x^2r_y^2r_z^2), \tag{30}$$

with the mean asymmetry $v = (v_1 + v_2)/2$ and the difference $\delta v = (v_1 - v_2)/2$. The existence of dipole and quadrupole asymmetries is plausible since it can be deduced from electric and elastic internal fields which couple weakly to an arbitrarily chosen defect. In contrast the octupole term has no such explanation and we hence neglect it in the following. The asymmetries V_d and V_q will be of the same order of magnitude as $4k_1k_2/J$. Treating them properly one is led to the following conclusions:

(i) We find that the part of the dipole mean asymmetry which is parallel to the distance vector $\vec{R}$ alters the frequency to $\sqrt{(4k_1k_2/J)^2 + v^2}$; this result is consistent with that proposed by Würger [4].

(ii) All other terms (such as the quadrupole terms) do not change the transition frequency; neither does the difference in asymmetry.

These results are shown in figure 7. In the middle we show the lowest multiplett without asymmetry; on the right hand side we show the 'dipole asymmetry' changing the energy levels, on the left hand side we show the 'quadrupole asymmetry' simply shifting the levels without changing the frequencies of the allowed transitions. The experiments by Weis are hence only sensitive to the *mean dipole asymmetry*. All other forms of asymmetry do not play a significant role here.

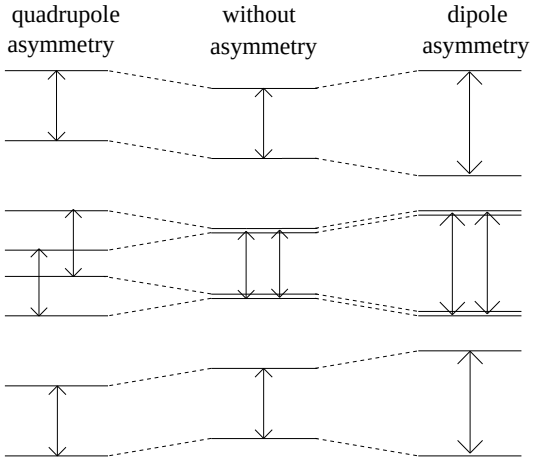

Figure 7: The lowest multiplett of NN2

5 Conclusion

In this article we had the aim to compare the physics of a two-level-system (TLS) to that of an eight-state-system (ESS). Both systems are used as possible models for cubic substitutional defects such as the lithium atom in a KCl host lattice. The ESS reflects much better our microscopic picture of the defect and it is hence interesting to know what features are left out of consideration when treating the defect as a TLS.

Using a tensorial notation we reminded the reader that the ESS reduces to three TLS if tunneling along the face and space diagonal of the cube is neglected. Then we presented three contexts

where differences between the two models arise. First we looked at the temperature dependence of the specific heat and the static dielectric susceptibility. A simple way to summarize the differences of the models is to state that for the TLS the relation $k^2\,\partial_T\chi \;=\; c_v$ holds, whereas this is not true for the ESS. In particular the maximum temperature of specific heat and the turning point of the susceptibility coincide for the TLS, whereas they are different for the ESS. We think that the experimental data indeed shows this tendency. The ratio f/k (face to edge tunneling) and the isotope effect ${}^6k/\,{}^7k$ estimated from the data leads to reasonable orders of magnitude for the barrier height (100-200K).

Second we investigated the differences of the two models in the presence of external forces (uniaxial pressure and static electric field). There appear different aspects where tunneling along the face and space diagonal of the cube is visible. These features make it possible to set up a resonance experiment where the face diagonal tunneling can be measured directly: applying the electric field along the [111]–direction, there are (both acoustic and electromagnetic) transitions with frequencies $\omega \sim f(pF)^2/((pF)^2+k^2)$ (where p denotes the dipole moment and F the static electric field). Of course such features cannot be described within the framework of a TLS.

As a third context we discussed strongly coupled defect pairs. Here again some properties arise that cannot be explained by a two-level-approximation. For strongly coupled pairs *geometric* selection rules inhibit transitions for some constellations (such as the nearest neighbors). In addition different asymmetry terms are possible for an ESS, whereas in the TLS only one such term appears. It is by the interplay of selection rules and the structure of the spectrum, that these other asymmetries are not observable in the echo experiments performed. This is why the situation can be described in terms of an effective TLS.

We thus conclude that there is a number of situations where the ESS shows observable features which cannot be described by a TLS. Nevertheless the latter is a good approximation in all contexts where the geometry and the parameters for tunneling along the face and space diagonal are of no relevance. In these situations the TLS being the simplest model for a tunneling degree of freedom indeed sketches all essential features of the defect.

ACKNOWLEDGEMENTS We wish to acknowledge helpfull discussions with C. Enss, H. Horner, B. Thimmel and A. Würger.

References

[1] V. Narayanamurti, R.O. Pohl: Rev. Mod. Phys. 42, 201 (1970)

[2] J.P. Harrison, P.P. Peressini, R.O. Pohl: Phys. Rev. B171, 1037 (1968)

[3] L.D. Landau, E.M. Lifschitz: Lehrbuch der theoretischen Physik, Band VII Elastizitätstheorie, Akademie-Verlag Berlin (1983)

[4] A. Würger: From Coherent Tunneling to Relaxation, Springer Tracts in Modern Physics 135, Springer Heidelberg (1996)

[5] M. Gomez, S.P. Bowen, J.A. Krumhansl: Phys. Rev. B153, 1009 (1967)

[6] C. Enss, M. Gaukler, S. Hunklinger, M. Tornow, R. Weis, A. Würger: eingereicht bei Phys. Rev. B (1995)

[7] R. Kubo, M. Toda, N. Hashistume: Statistical Physics, Springer Heidelberg (1985)

[8] A.T. Fiory: Phys. Rev. B 4, 614 (1971)

[9] R. Weis, C. Enss, A. Würger, F. Lüty: Preprint: Coherent Tunneling of Lithium Defect Pairs in KCl Crystals (1996)

[10] O. Terzidis, A. Würger: Journal of Physics Cond. Matt. 8 7303 (1996); Z. Phys. B94, 341-346 (1994)

[11] M.W. Klein, Z.H. Wang: Phys. Rev. Lett. 57, 1355 (1986); M.W. Klein: Phys. Rev. B29, 5825 (1984)

[12] P. Nalbach: Diploma thesis, Ruprecht-Karls-Universität Heidelberg 1996 (unpublished)